Immune modulation to improve survival of respiratory virus infections in mice

Authors: Shradha Wali[1,2], Jose R. Flores[2], Ana Maria Jaramillo[2], David L. Goldblatt[2], Jezreel Pantaleón García[2], Michael J. Tuvim[2], Burton F. Dickey[2], Scott E. Evans[1,2]

Author affiliations: [1]University of Texas MD Anderson Cancer Center UTHealth Graduate School of Biomedical Sciences, Houston Texas 77030

[2]University of Texas MD Anderson Cancer Center, Department of Pulmonary Medicine, Houston Texas 77030

To whom correspondence should be addressed: Scott E. Evans, M.D.

6565 MD Anderson Blvd

Houston TX 77030

Email: seevans@mdanderson.org

Telephone: 713-563-7433

Author contributions: S.W. designed and performed the experiments, analyzed the data, and wrote the manuscript. J.R.F., A.M.J., D.L.G. and J.P.G performed experiments. M.J.T., B.F.D. conceptualized the project and critically reviewed the data. S.E.E. conceptualized the project, designed experiments, provided critical evaluation of data and edited the manuscript. [1]

[1] This study was supported by NIH grants R01 HL117976, DP2 HL123229 and R35 HL144805 to S.E.E.

Running Title: Epithelial defence against viral immunopathology

Abstract

Viral pneumonia remains a global health threat requiring novel treatment strategies, as strikingly exemplified in the SARS-CoV-2 pandemic of 2019-2020. We have reported that mice treated with a combination of inhaled Toll-like receptor (TLR) 2/6 and TLR 9 agonists (Pam2-ODN) to stimulate innate immunity are broadly protected against respiratory pathogens, but the mechanisms underlying this protection remain incompletely elucidated. Here, we show in a lethal paramyxovirus model that Pam2-ODN-enhanced survival is associated with robust virus inactivation by reactive oxygen species (ROS), which occurs prior to internalization by lung epithelial cells. However, we also found that mortality in sham-treated mice temporally corresponded with $CD8^+$ T cell-enriched lung inflammation that peaks on days 11-12 after viral challenge, when the viral burden has waned to a scarcely detectable level. Pam2-ODN treatment blocked this injurious inflammation by reducing the viral burden, and alternatively, depleting $CD8^+$ T cells 8 days after viral challenge also decreased mortality. These findings reveal opportunities for targeted immunomodulation to protect susceptible individuals against the morbidity and mortality of respiratory viral infections.

Keywords: Immunomodulation, immunopathology, $CD8^+$ T cells, viral pneumonia, inducible epithelial resistance

Introduction

Viruses are the most frequent cause of community acquired pneumonia in children and adults, resulting in significant morbidity in vulnerable subjects and exerting a tremendous health care burden (1-5). Seasonal influenza and emergent pandemic viruses, such as SARS-CoV-2, inflict particular mortality in susceptible individuals, with clinicians frequently lacking effective interventions to improve patient outcomes (6-9). Moreover, in addition to causing acute disease, respiratory virus infections are often complicated by chronic lung pathologies, such as asthma induction, progression and exacerbation (10-12). Therefore, development of novel therapeutic anti-viral strategies is required to effectively prevent and treat respiratory infections and their associated chronic complications (13, 14).

While lung epithelial cells are the principal targets of most respiratory viruses (15), there is expanding evidence that lung epithelia themselves are capable of generating anti-microbial responses (12, 16, 17). We hypothesized that lung epithelial cells can be harnessed to control virus replication, thereby enhancing acute survival and reducing chronic complications of virus infections (18-21). Our group has previously described the phenomenon of inducible epithelial resistance wherein the lungs' mucosal defenses can be broadly stimulated to protect against a wide range of respiratory pathogens, including viruses (18-23). This protection is induced by a single inhalation of a combination treatment consisting of Toll like receptor (TLR) 2/6 and 9 agonists (Pam2-ODN) shortly before or after viral challenge. While no individual leukocyte populations have been identified as critical for Pam2-ODN-induced resistance, lung epithelial cells are essential to the inducible anti-viral response (18). Further, we have shown that

Pam2-ODN mediated protection is dependent upon epithelial generation of reactive oxygen species (ROS) but, interestingly, does not require Type I interferons (22, 23). More recently, we have shown prevention of chronic virus-induced asthma in mice treated with Pam2-ODN but we have not clarified the anti-viral mechanisms (24).

In this study, we investigated the mechanisms of Pam2-ODN enhanced mouse survival of pneumonia caused by a paramyxovirus, Sendai virus (SeV). We found that Pam2-ODN treatment not only reduced lung SeV burden but also decreased epithelial cell injury and host immunopathologic leukocyte responses to SeV infections. While $CD8^+$ T cells are known to contribute to anti-viral immunity, it is shown here that $CD8^+$ T cells contribute substantially to mortality, and this effect can be prevented by Pam2-ODN treatment early in the course of infection or $CD8^+$ depletion late in the course. Further, we demonstrate anti-viral mechanisms of inducible epithelial resistance, where virus particles are inactivated in a ROS-dependent manner prior to internalization by their epithelial targets.

Materials and Methods

Mice: All *in vivo* experiments were performed using 6- to 10-week-old C57BL/6J mice of a single sex and were handled according to the Institutional Animal Care and Use Committee of MD Anderson Cancer Center, protocol 00000907-RN01.

Cells: Mouse lung epithelial (MLE-15) cells were kindly provided by Jeffrey Whitsett, Cincinnati Children's Hospital Medical Center. Mouse tracheal epithelial cells were harvested and cultured as previously described (22, 25). See *Supplemental Methods* for additional details.

TLR treatments and viral challenges: Cells were treated with $Pam2CSK_4$ (2.2 µM) and ODN M362 (0.55 µM) as previously described (22, 23). Mice were treated with 10 ml of $Pam2CSK_4$ (4 µM) and ODN M362 (1 µM) by nebulization as previously described (22, 23). For *in vitro* challenges, SeV at multiplicity of infection (MOI) = 1 was used. Unless otherwise stated, mice were challenged with 1×10^8 plaque forming units (pfu) inserted into the oropharynx as described (24). See *Supplemental Methods* for additional details.

Flow cytometry: Single cells from disaggregated lungs or cell culture were stained as indicated in the antibody table (Table 1), fixed, and acquired on a BD LSRII (BD Biosciences). See *Supplemental Methods* for additional details.

Epithelial proliferation assays: Epithelial proliferation was determined by staining lung sections for EdU 24 h after intraperitoneal injection. See Supplemental *Methods* for details.

$CD8^+$ T cell depletion: Anti-CD8-β antibody (200 µg/mouse, clone 53-5.8, Bioxell) was delivered to mice intraperitoneally at indicated time points. $CD8^+$ T cell depletion was confirmed by flow cytometry analysis 24 to 48 h after depletion.

Viral burden quantification: Viral burden was determined by reverse transcription quantitative PCR (RT-qPCR) of the Sendai Matrix (M) protein normalized to host house-keeping gene 18SRNA. For *in vivo* experiments, mouse lungs were collected 5 days after SeV challenge. For in vitro experiments, cell lysates were collected 24 h after infection, unless otherwise indicated. See *Supplemental Methods* for additional details.

ROS inhibition *in vitro* and *in vivo*: NADPH oxidase activity was inhibited using GKT137831 (Selleckchem). Mitochondrial ROS production was inhibited using the combination of FCCP (Cayman Chemicals) and TTFA (Cayman Chemicals). See *Supplemental Methods* for additional details.

Viral attachment assays: For most enveloped viruses, internalization into epithelial cells is inhibited at 4º C without affecting viral binding to epithelial cells (26-28). MLE-15 cells were infected with SeV at 4º C for 4 h, washed to remove unattached virus, then assessed for uninternalized SeV burden using immunofluorescence or flow cytometry. See *Supplemental Methods* for additional details.

Results

Enhanced mouse survival of SeV infection by Pam2-ODN treatment

Aerosolized Pam2-ODN treatment one day prior to SeV challenge increased mouse survival of SeV challenge (Figure 1A), similar to the protection observed against lethal influenza pneumonia (18, 21, 22). The survival benefit was associated with reduced lung SeV burden, as measured by SeV M gene expression (Figure 1B). Investigating the natural progression of infection revealed that SeV lung burden was maximal on day 5 and gradually decreased until falling below the limit of quantification (LOQ) by day 11 (Figure 1C). Pam2-ODN pretreatment reduced SeV burden on all assessed days (Figure 1C). Although the lethality of SeV infection was exquisitely dependent on the inoculum size, we strikingly found that peak mortality paradoxically occurred around days 10 to 12 after infection irrespective of inoculum size, despite the fact that SeV is essentially undetectable that long after challenge (Figure 1A, C, and D).

Pam2-ODN treatment attenuates SeV-induced epithelial injury

This temporal dissociation between peak virus burden and peak mortality led to the hypothesis that SeV-induced mortality may not be exclusively driven by excessive virus burden but may also result from untoward SeV-induced host immune response. Therefore, the acute changes in mouse lungs following SeV infection were characterized. We found increases in lung epithelial cleaved caspase 3 (cCasp3), a marker for programmed cell death, on days 7 to 11 after SeV infection (Figure 2A, upper panel). Virus infection-related epithelial cell injury and death is typically associated with

proliferative repair mechanisms (29, 30). Staining the infected mouse lung tissue for Ki67 and EdU revealed maximum signals for both markers in the second week after infection (Figure 2B-E, upper panel). These events of lung epithelial cell death and proliferation coincided with the peak of mortality (day 12, Figure 1E). Further, hematoxylin and eosin staining of lung tissues infected with SeV showed profound increases in inflammatory cells from days 7 to 10 with evidence of damaged airway and parenchymal tissue (Figure 2F). However, Pam2-ODN pretreatment of mice reduced epithelial cell injury and proliferation (Figure 2A-E, lower panel). This temporal association of epithelial injury and death after viral clearance supported our hypothesis that mouse mortality caused by SeV infection is due in part to the host immune response to SeV infections.

Pam2-ODN attenuates SeV-induced lymphocytic lung inflammation.

To explore this hypothesis, the host leukocyte response to SeV infection was characterized. Differential Giemsa staining of bronchoalveolar lavage (BAL) cells revealed increased neutrophils on days 2 to 5 and increased macrophages on days 5 to 8 (Figure 3A, left and middle panel, solid grey line) after SeV challenge. Congruent with our prior studies, inhaled treatment with Pam2-ODN in the absence of infection led to a rapid rise in neutrophils that was resolved within 5 days (Figure 3A, dashed line) (31). The neutrophil response to SeV challenge was modestly increased among mice pretreated with Pam2-ODN (Figure 3A, left panel, solid dark line). Pam2-ODN-treated, SeV-challenged mice showed almost no difference in macrophage number compared to PBS-treated, SeV-challenged mice (Figure 3A, middle panel, solid dark line). A rise in

lymphocytes was observed on days 8 to 11 in PBS-treated, SeV-challenged mice (Figure 3A, right panel, solid grey line), temporally corresponding with peak mortality. However, Pam2-ODN treated, SeV-challenged mice displayed significantly reduced lymphocyte numbers at every time point assessed (Figure 3A, right panel, solid dark line). The gating strategy for lymphocyte subsets by flow cytometry is shown in Supplementary Figure 1. A modest reduction in $CD4^+$ T cells was observed in Pam2-ODN-treated, SeV-challenged mice compared to PBS-treated, SeV-challenged mice (Supplementary Figure 2). We also found the percentage of $CD19^+$ $B220^+$ B cells reduced after SeV infection in comparison to Pam2-ODN treated and uninfected mice (Supplementary Figure 2), as has been seen with other viral models (32, 33). However, the biggest difference between groups was in $CD8^+$ T cells, with Pam2-ODN-treated, SeV-challenged mice displaying a significantly lower number and percentage of $CD8^+$ T cells than PBS treated, SeV-challenged mice (Figure 3B, C). Since the greatest difference after Pam2-ODN treatment was in $CD8^+$ T cell levels and there was a tight correlation between peak mortality and the increase in lung $CD8^+$ T cells on days 8 to 11, we investigated the role of $CD8^+$ T cells in SeV-induced mortality.

Depleting $CD8^+$ T cells after viral clearance enhances survival of SeV infection

To understand the apparent contributions of host immunopathology to mouse outcomes, we depleted $CD8^+$ T cells on day 8 -- after virus burden was substantially reduced but before peak mouse mortality (Figures 1 and 4A). Mice depleted of $CD8^+$ T cells displayed significantly enhanced survival of SeV challenge compared to mice with intact $CD8^+$ T cells (Figure 4B). Depletion of $CD8^+$ T cells was confirmed by flow

cytometry in disaggregated lung cells 10 days after SeV challenge (Figure 4C, Supplementary Figure 3A). We also assessed lung injury by hematoxylin and eosin staining of lung tissue 10 days after SeV challenge and found increased inflammation and epithelial cell damage in undepleted mice compared to $CD8^+$ T cell-depleted mice (Figure 4D). This supported our hypothesis that $CD8^+$ T cells contribute to fatal SeV-induced immunopathology.

To assess the role of $CD8^+$ T cells throughout the course of infection, mouse $CD8^+$ T cells were depleted prior to and during SeV challenge (Figure 4A, Supplementary Figure. 3A, B). This depletion resulted in significantly reduced survival of SeV infection (Supplementary Figure 3C), compatible with the known antiviral functions of $CD8^+$ T cells (34-36). However, it is notable that Pam2-ODN treatment still significantly enhanced survival of SeV challenge even in the absence of $CD8^+$ T cells (Supplementary Figure 3C). This finding was congruent with our previous studies showing Pam2-ODN inducible resistance against bacterial pneumonia despite the lack of mature lymphocytes (*Rag1*$^{-/-}$) (18).

Pam2-ODN treatment leads to extracellular inactivation of virus particles

As the antiviral protection consistently correlated with reduced viral burden *in vivo*, and as the reduced virus burden likely contributes to the reduced $CD8^+$ T cell levels, we sought to determine how Pam2-ODN-induced responses cause antiviral effects. Assessing the effect of Pam2-ODN on SeV burden in immortalized mouse epithelial

cells (MLE-15) and primary mouse tracheal epithelial cells (mTEC), we found that Pam2-ODN treatment reduced SeV burden at every time point measured, reflecting the inducible antiviral capacity of isolated epithelial cells (Supplementary Figure 4). Further, we investigated whether the principal Pam2-ODN effect occurred before (extracellular) or after (intracellular) virus internalization into their epithelial targets. SeV inoculation was carried out at 4º C preventing SeV internalization while allowing SeV attachment to epithelial cells (26-28). Using multiple methods to determine the effect of Pam2-ODN on SeV attachment, we found no differences in attachment (Figure 5A-D). However, even though similar numbers of virus particles were attached to epithelial cells, when these attached virus particles were liberated from the epithelial cell targets, virus particles from Pam2-ODN-treated epithelial cells were less able to subsequently infect other naive epithelial cells (Figure 5E, F). As the number of attached virus particles was the same, this difference in SeV burden in cells that received liberated virus particles from PBS vs Pam2-ODN treated cells indicated that SeV is inactivated prior to epithelial internalization.

Pam2-ODN-induced epithelial ROS protect against SeV infection and $CD8^+$ T cell immunopathology

The anti-influenza response initiated by Pam2-ODN requires epithelial generation of ROS from both NADPH-dependent dual oxidase and mitochondrial sources (22, 23). Extending these findings to the SeV model, an NADPH oxidase inhibitor (GKT 137831) fully abrogated the Pam2-ODN-induced anti-SeV response (Figure 6A). Similarly, treatment with a combination of FCCP (an uncoupler of oxidative phosphorylation) and

TTFA (a complex II inhibitor) obviated the Pam2-ODN-induced anti-SeV response (Figure 6B) (22, 23). Further, it was found that Pam2-ODN induced epithelial generation of ROS were required for inactivation of SeV prior to epithelial entry (Figure 6C). Congruent with these *in vitro* and *ex vivo* studies, mice treated with FCCP and TTFA before Pam2-ODN treatment and SeV challenge (Figure 6D) demonstrated reduced survival (Figure 6E), increased SeV burden (Figure 6F), and increased $CD8^+$ T cells on day 10 (Figure 6G).

Discussion

In this study, we demonstrate that therapeutic stimulation of lung epithelial cells enhances mouse survival of acute SeV infections by both reducing the virus burden and attenuating host immunopathology. While our group has demonstrated inducible resistance against multiple respiratory pathogens including viruses (18-23, 31), these studies demonstrate for the first time when in the virus lifecycle the anti-viral effects begin (viz., prior to internalization), and substantiate the role of ROS in protection against SeV.

While Pam2-ODN treatment provided a significant host survival benefit in SeV infection, we observed this survival benefit occurring after the time when PBS-treated mice had cleared the virus. This observation prompted the hypothesis that host mortality is not the exclusive result of direct viral injury to the lungs, but due at least in part to the host response to the virus infections. We observed enhanced survival of SeV infections in

mice depleted of $CD8^+$ T cells 8 days after infection (Figure 4A,B), revealing the importance of balancing the dual functions of $CD8^+$ T cells in anti-viral immunity and in causing fatal immunopathology. Our findings suggest that the surge in $CD8^+$ T cells within the lungs after most virus has been cleared causes physiologic impairment via lung injury and cell death (Figure 4D). These observations demonstrate an advantage of early immune stimulation to enhance viral clearance and late immune suppression to prevent immunopathology and enhance overall outcome of respiratory infections. This is potentially informative in the context of treating pneumonia in immunocompromised patients, and is likely applicable to broader clinical populations, including those suffering lung injury associated with SARS-CoV-2. Based on this reasoning, clinical trials of the use of Pam2-ODN to prevent or treat early COVID-19 have been launched (NCT04313023, NCT04312997), and we suggest that therapeutic targeting of $CD8^+$ T cells later in COVID-19 be considered.

Previous reports support the concept of counter-balanced immune protection and immunopathology by $CD8^+$ T cells during virus infections (36-41). Some reports have shown that antigen-experienced memory $CD8^+$ T cells enhance respiratory syncytial virus (RSV) clearance, but also mediate severe immunopathology (39, 42). However, our study is the first to demonstrate the survival advantage in paramyxovirus respiratory infection of either stimulating the lungs' mucosal defenses early in the infection or of suppressing the $CD8^+$ T cells later in the infection. Our findings are also congruent with reports on the role of $CD8^+$ T cells in non-respiratory viral infection models, such as in West Nile virus infection, where $CD8^+$ T cell deficient mice display decreased mortality

285 (40). While findings from that study and others reveal that the harmful effects of $CD8^+$ T
286 cell mediated immunopathology may supersede the benefits of T cell mediated viral
287 clearance, the question arises of what might be the adaptive value of the vigorous late
288 $CD8^+$ T cell response. One possibility is that it might ensure that the infection does not
289 flare again, but that seems implausible since the host has successfully defended itself
290 against the initial infection, and innate immune mechanisms presumably remain intact
291 and are possibly primed (43, 44), in addition to the multiple adaptive immune
292 mechanisms that increasingly come into play. The possibility that the immunopathology
293 simply results from an error on the part of the immune system also seems implausible in
294 view of the substantial rate of host mortality, suggesting there is likely an adaptive value
295 to the response. A third possibility, that the persistence of pockets of low level infection
296 might lead to chronic lung pathology, is supported by a recent study showing that sites
297 of viral RNA remnants following influenza infection are linked to chronic lung disease
298 (45). Thus, a trade-off may exist between the adaptive value of a vigorous $CD8^+$ T cell
299 response to prevent chronic lung disease and the acute mortality it can cause.
300 Manipulating this balance therapeutically will need to account for both the benefits and
301 costs of the response. It is particularly appealing to develop inducible anti-microbial
302 strategies that do not rely on conventional T cell-mediated microbial clearance and are
303 also effective in vulnerable immune deficient populations (18, 22, 25, 46).

304

305 Although the $CD8^+$ T cell depletion studies enhanced our understanding of
306 immunopathology in virus infections, much of the survival benefit against SeV infection
307 was mediated by rapid anti-viral effects induced by Pam2-ODN. This led us to

investigate the mechanisms of these inducible anti-viral effects. Given the multiple steps in the virus life cycle, it was not known at what stage Pam2-ODN exerted its anti-viral effect. Exploring this, we found no difference in number of SeV particles attached to the cells between PBS and Pam2-ODN treatment (Figure 5A-D). However, attached virus particles that were liberated from Pam2-ODN treated cells retained less infective capacity when added to naïve epithelial cells, revealing pre-internalization virus inactivation by Pam2-ODN treatment (Figure 5E, F).

Knowing that Pam2-ODN inducible resistance required ROS production to protect against influenza (22), we studied the role of ROS in Pam2-ODN-mediated reduction in SeV burden. ROS inhibition not only led to attenuation of Pam2-ODN's anti-viral effect but allowed increased lung $CD8^+$ T cell numbers, implicating Pam2-ODN-induced ROS in preventing both identified mechanisms of mouse mortality in SeV pneumonia (Figure 6). ROS inhibition led to loss of Pam2-ODN-inducible *in vitro* inactivation of SeV prior to epithelial internalization (Figure 6C), demonstrating for the first time that epithelial ROS directly contribute to virus inactivation.

Production of ROS as a microbicidal mechanism has been widely reported in phagocytic cells (47-49). However, this mechanism has not been extensively studied in non-phagocytic cells (50), where it apparently acts predominantly extracellularly rather than intracellularly as in phagocytes. (Figure 5F, G). These findings of viral inactivation

by epithelial ROS production reveal an essential component of inducible epithelial resistance.

Taken together, these findings provide mechanistic insights into the antiviral responses generated by the lung epithelium and the prevention of host immunopathology that may inform future therapeutics to target immunomodulation as a means to improve the survival of respiratory infections in vulnerable populations.

Acknowledgments and Disclosures:

The authors would like to thank Dr. Yongxing Wang for optimization of ROS inhibition experiments. M.J.T., B.F.D., and S.E.E. are authors on U.S. patent 8,883,174, "Stimulation of Innate Resistance of the Lungs to Infection with Synthetic Ligands." M.J.T., B.F.D., and S.E.E. own stock in Pulmotect, Inc., which holds the commercial options on these patent disclosures. All other authors declare that no conflict of interest exists.

References:

1. Mizgerd JP. Lung infection--a public health priority. *PLoS medicine* 2006;3(2):e76.

2. Luckhaupt SE, Sweeney MH, Funk R, Calvert GM, Nowell M, D'Mello T, Reingold A, Meek J, Yousey-Hindes K, Arnold KE, et al. Influenza-associated

hospitalizations by industry, 2009-10 influenza season, united states. *Emerging infectious diseases* 2012;18(4):556-562.

3. Thompson WW, Shay DK, Weintraub E, Brammer L, Cox N, Anderson LJ, Fukuda K. Mortality associated with influenza and respiratory syncytial virus in the united states. *Jama* 2003;289(2):179-186.

4. Jain S, Self WH, Wunderink RG, Fakhran S, Balk R, Bramley AM, Reed C, Grijalva CG, Anderson EJ, Courtney DM, et al. Community-acquired pneumonia requiring hospitalization among u.S. Adults. *N Engl J Med* 2015;373(5):415-427.

5. Jain S, Williams DJ, Arnold SR, Ampofo K, Bramley AM, Reed C, Stockmann C, Anderson EJ, Grijalva CG, Self WH, et al. Community-acquired pneumonia requiring hospitalization among u.S. Children. *N Engl J Med* 2015;372(9):835-845.

6. Fauci AS, Lane HC, Redfield RR. Covid-19 - navigating the uncharted. *N Engl J Med* 2020;382(13):1268-1269.

7. Taubenberger JK, Kash JC, Morens DM. The 1918 influenza pandemic: 100 years of questions answered and unanswered. *Sci Transl Med* 2019;11(502).

8. Wang X, Li Y, O'Brien KL, Madhi SA, Widdowson MA, Byass P, Omer SB, Abbas Q, Ali A, Amu A, et al. Global burden of respiratory infections associated with seasonal influenza in children under 5 years in 2018: A systematic review and modelling study. *Lancet Glob Health* 2020;8(4):e497-e510.

9. Li Q, Guan X, Wu P, Wang X, Zhou L, Tong Y, Ren R, Leung KSM, Lau EHY, Wong JY, et al. Early transmission dynamics in wuhan, china, of novel coronavirus-infected pneumonia. *N Engl J Med* 2020;382(13):1199-1207.

10. Busse WW, Lemanske RF, Jr., Gern JE. Role of viral respiratory infections in asthma and asthma exacerbations. *Lancet* 2010;376(9743):826-834.

11. Folkerts G, Busse WW, Nijkamp FP, Sorkness R, Gern JE. Virus-induced airway hyperresponsiveness and asthma. *American journal of respiratory and critical care medicine* 1998;157(6 Pt 1):1708-1720.

12. Holtzman MJ, Byers DE, Brett JA, Patel AC, Agapov E, Jin X, Wu K. Linking acute infection to chronic lung disease. The role of il-33-expressing epithelial progenitor cells. *Annals of the American Thoracic Society* 2014;11 Suppl 5:S287-291.

13. Olin JT, Wechsler ME. Asthma: Pathogenesis and novel drugs for treatment. *Bmj* 2014;349:g5517.

14. Shaw DE, Green RH, Bradding P. Asthma exacerbations: Prevention is better than cure. *Therapeutics and clinical risk management* 2005;1(4):273-277.

15. Ibricevic A, Pekosz A, Walter MJ, Newby C, Battaile JT, Brown EG, Holtzman MJ, Brody SL. Influenza virus receptor specificity and cell tropism in mouse and human airway epithelial cells. *J Virol* 2006;80(15):7469-7480.

16. Byers DE, Alexander-Brett J, Patel AC, Agapov E, Dang-Vu G, Jin X, Wu K, You Y, Alevy Y, Girard JP, et al. Long-term il-33-producing epithelial progenitor cells in chronic obstructive lung disease. *The Journal of clinical investigation* 2013;123(9):3967-3982.

17. Leiva-Juarez MM, Kolls JK, Evans SE. Lung epithelial cells: Therapeutically inducible effectors of antimicrobial defense. *Mucosal immunology* 2018;11(1):21-34.

18. Cleaver JO, You D, Michaud DR, Pruneda FA, Juarez MM, Zhang J, Weill PM, Adachi R, Gong L, Moghaddam SJ, et al. Lung epithelial cells are essential effectors of inducible resistance to pneumonia. *Mucosal immunology* 2014;7(1):78-88.

19. Duggan JM, You D, Cleaver JO, Larson DT, Garza RJ, Guzman Pruneda FA, Tuvim MJ, Zhang J, Dickey BF, Evans SE. Synergistic interactions of tlr2/6 and tlr9 induce a high level of resistance to lung infection in mice. *Journal of immunology* 2011;186(10):5916-5926.

20. Evans SE, Tuvim MJ, Fox CJ, Sachdev N, Gibiansky L, Dickey BF. Inhaled innate immune ligands to prevent pneumonia. *British journal of pharmacology* 2011;163(1):195-206.

21. Tuvim MJ, Gilbert BE, Dickey BF, Evans SE. Synergistic tlr2/6 and tlr9 activation protects mice against lethal influenza pneumonia. *PLoS One* 2012;7(1):e30596.

22. Kirkpatrick CT, Wang Y, Leiva Juarez MM, Shivshankar P, Pantaleon Garcia J, Plumer AK, Kulkarni VV, Ware HH, Gulraiz F, Chavez Cavasos MA, et al. Inducible lung epithelial resistance requires multisource reactive oxygen species generation to protect against viral infections. *mBio* 2018;9(3).

23. Ware HH, Kulkarni VV, Wang Y, Pantaleon Garcia J, Leiva Juarez M, Kirkpatrick CT, Wali S, Syed S, Kontoyiannis AD, Sikkema WKA, et al. Inducible lung epithelial resistance requires multisource reactive oxygen species generation to protect against bacterial infections. *PLoS One* 2019;14(2):e0208216.

24. Goldblatt DL, Flores JR, Valverde Ha G, Jaramillo AM, Tkachman S, Kirkpatrick CT, Wali S, Hernandez B, Ost DE, Scott BL, et al. Inducible epithelial resistance against

415 acute sendai virus infection prevents chronic asthma-like lung disease in mice. *British*
416 *journal of pharmacology* 2020.
417 25. Leiva-Juarez MM, Ware HH, Kulkarni VV, Zweidler-McKay PA, Tuvim MJ, Evans
418 SE. Inducible epithelial resistance protects mice against leukemia-associated
419 pneumonia. *Blood* 2016;128(7):982-992.
420 26. Tscherne DM, Jones CT, Evans MJ, Lindenbach BD, McKeating JA, Rice CM.
421 Time- and temperature-dependent activation of hepatitis c virus for low-ph-triggered
422 entry. *J Virol* 2006;80(4):1734-1741.
423 27. Haywood AM, Boyer BP. Sendai virus membrane fusion: Time course and effect
424 of temperature, ph, calcium, and receptor concentration. *Biochemistry*
425 1982;21(24):6041-6046.
426 28. Tai CJ, Li CL, Tai CJ, Wang CK, Lin LT. Early viral entry assays for the
427 identification and evaluation of antiviral compounds. *J Vis Exp* 2015(105):e53124.
428 29. Hines EA, Szakaly RJ, Leng N, Webster AT, Verheyden JM, Lashua AJ,
429 Kendziorski C, Rosenthal LA, Gern JE, Sorkness RL, et al. Comparison of temporal
430 transcriptomic profiles from immature lungs of two rat strains reveals a viral response
431 signature associated with chronic lung dysfunction. *PLoS One* 2014;9(12):e112997.
432 30. Look DC, Walter MJ, Williamson MR, Pang L, You Y, Sreshta JN, Johnson JE,
433 Zander DS, Brody SL. Effects of paramyxoviral infection on airway epithelial cell foxj1
434 expression, ciliogenesis, and mucociliary function. *Am J Pathol* 2001;159(6):2055-2069.
435 31. Alfaro VY, Goldblatt DL, Valverde GR, Munsell MF, Quinton LJ, Walker AK,
436 Dantzer R, Varadhachary A, Scott BL, Evans SE, et al. Safety, tolerability, and

biomarkers of the treatment of mice with aerosolized toll-like receptor ligands. *Front Pharmacol* 2014;5:8.

32. Bekker V, Scherpbier H, Beld M, Piriou E, van Breda A, Lange J, van Leth F, Jurriaans S, Alders S, Wertheim-van Dillen P, et al. Epstein-barr virus infects b and non-b lymphocytes in hiv-1-infected children and adolescents. *J Infect Dis* 2006;194(9):1323-1330.

33. Shearer WT, Easley KA, Goldfarb J, Rosenblatt HM, Jenson HB, Kovacs A, McIntosh K. Prospective 5-year study of peripheral blood cd4, cd8, and cd19/cd20 lymphocytes and serum igs in children born to hiv-1 women. The p(2)c(2) hiv study group. *J Allergy Clin Immunol* 2000;106(3):559-566.

34. Cannon MJ, Stott EJ, Taylor G, Askonas BA. Clearance of persistent respiratory syncytial virus infections in immunodeficient mice following transfer of primed t cells. *Immunology* 1987;62(1):133-138.

35. Graham BS, Bunton LA, Wright PF, Karzon DT. Role of t lymphocyte subsets in the pathogenesis of primary infection and rechallenge with respiratory syncytial virus in mice. *The Journal of clinical investigation* 1991;88(3):1026-1033.

36. Schmidt ME, Varga SM. Cytokines and cd8 t cell immunity during respiratory syncytial virus infection. *Cytokine* 2018.

37. Duan S, Thomas PG. Balancing immune protection and immune pathology by cd8(+) t-cell responses to influenza infection. *Front Immunol* 2016;7:25.

38. Hou S, Doherty PC, Zijlstra M, Jaenisch R, Katz JM. Delayed clearance of sendai virus in mice lacking class i mhc-restricted cd8+ t cells. *Journal of immunology* 1992;149(4):1319-1325.

460 39. Schmidt ME, Knudson CJ, Hartwig SM, Pewe LL, Meyerholz DK, Langlois RA,
461 Harty JT, Varga SM. Memory cd8 t cells mediate severe immunopathology following
462 respiratory syncytial virus infection. *PLoS Pathog* 2018;14(1):e1006810.
463 40. Wang Y, Lobigs M, Lee E, Mullbacher A. Cd8+ t cells mediate recovery and
464 immunopathology in west nile virus encephalitis. *J Virol* 2003;77(24):13323-13334.
465 41. Connors TJ, Ravindranath TM, Bickham KL, Gordon CL, Zhang F, Levin B, Baird
466 JS, Farber DL. Airway cd8(+) t cells are associated with lung injury during infant viral
467 respiratory tract infection. *Am J Respir Cell Mol Biol* 2016;54(6):822-830.
468 42. Cannon MJ, Openshaw PJ, Askonas BA. Cytotoxic t cells clear virus but
469 augment lung pathology in mice infected with respiratory syncytial virus. *J Exp Med*
470 1988;168(3):1163-1168.
471 43. Kaufmann E, Sanz J, Dunn JL, Khan N, Mendonca LE, Pacis A, Tzelepis F,
472 Pernet E, Dumaine A, Grenier JC, et al. Bcg educates hematopoietic stem cells to
473 generate protective innate immunity against tuberculosis. *Cell* 2018;172(1-2):176-190
474 e119.
475 44. Netea MG, Joosten LAB. Trained immunity and local innate immune memory in
476 the lung. *Cell* 2018;175(6):1463-1465.
477 45. Keeler SP, Agapov EV, Hinojosa ME, Letvin AN, Wu K, Holtzman MJ. Influenza
478 a virus infection causes chronic lung disease linked to sites of active viral rna remnants.
479 *Journal of immunology* 2018;201(8):2354-2368.
480 46. Evans SE, Xu Y, Tuvim MJ, Dickey BF. Inducible innate resistance of lung
481 epithelium to infection. *Annu Rev Physiol* 2010;72:413-435.

47. Forman HJ, Torres M. Reactive oxygen species and cell signaling: Respiratory burst in macrophage signaling. *American journal of respiratory and critical care medicine* 2002;166(12 Pt 2):S4-8.

48. Huang J, Canadien V, Lam GY, Steinberg BE, Dinauer MC, Magalhaes MA, Glogauer M, Grinstein S, Brumell JH. Activation of antibacterial autophagy by nadph oxidases. *Proc Natl Acad Sci U S A* 2009;106(15):6226-6231.

49. Yang CS, Shin DM, Kim KH, Lee ZW, Lee CH, Park SG, Bae YS, Jo EK. Nadph oxidase 2 interaction with tlr2 is required for efficient innate immune responses to mycobacteria via cathelicidin expression. *Journal of immunology* 2009;182(6):3696-3705.

50. Paiva CN, Bozza MT. Are reactive oxygen species always detrimental to pathogens? *Antioxid Redox Signal* 2014;20(6):1000-1037.

503 **Table 1**

Antibodies	Vendor	Catalogue numbers
CD3	Tonbo	65-0031-U100
CD4	Tonbo	60-0042-U100
CD8	Tonbo	25-0081-U100
Live dead	Tonbo	13-0870-T500
CD25	Biolegend	102038
Foxp3 Treg kit	eBiosciences	72-5775
CD8-Depleting Ab	Bioxell	BE0223-A025
CD19	Biolegend	115507
B220	BD Biosciences	562922
Anti-SeV virus Ab	MBL International	PD029
Ki67	Invitrogen	MA5-14520
cCasp3	Cell signaling	9662S

504

505

506 **Figure Legends**

507 **Figure 1**. **Pam2-ODN enhances mouse survival of SeV infection and reduces lung**
508 **virus burden. (A)** Survival of mice treated with PBS or Pam2-ODN one day prior to
509 SeV virus challenge. **(B)** Mouse lung SeV burden 5 days after infection assessed by
510 qPCR for Sendai Matrix (M) gene (Relative quantification, RQ to 18S) relative to 18S.

(C) Time course of lung SeV burden in mice treated with PBS or Pam2-ODN. **(D)** SeV inoculum dependent mouse survival. Data are representative from three independent experiments. n=10 mice per group in survival plots, n=4 mice/group in virus burden experiments. LOQ, limit of quantification. *p<0.05, **p<0.005.

Figure 2. **Pam2-ODN pretreatment reduces epithelial cell death and proliferation during acute SeV infection.** Cleaved caspase 3 (cCasp3) **(A)** or Ki67 **(B)** positive cells in mouse lung epithelium after SeV infection with or without Pam2-ODN treatment (lower panel). EdU positive cells in axial **(C)**, small airways **(D)** and parenchyma **(E)** after SeV infection with or without Pam2-ODN (lower panel). **(F)** Mouse lung histology following SeV challenge with or without Pam2-ODN. n=5 mice per condition. Data are representative from two independent experiments. Scale bar = 100 µm. *p<0.05.

Figure 3. **Pam2-ODN pretreatment reduces SeV induced lung $CD8^+$ T cells. (A)** Differential Giemsa staining of BAL cells from mice challenged with SeV with or without Pam2-ODN pretreatment. **(B)** Flow cytometry for $CD8^+$ T cells from disaggregated mouse lungs 11 days after SeV infection with or without Pam2-ODN. **(C)** Lung $CD8^+$ T cells 11 days after SeV challenge in mice pretreated with PBS or Pam2-ODN. Data are representative of three independent experiments for (A) and of five independent experiments for (B) and (C). *p<0.05 compared to PBS+SeV

Figure 4. Pam2-ODN treatment reduces $CD8^+$ T cell associated SeV induced immunopathology. Experimental outline **(A)**, survival **(B)** and percentage of $CD8^+$ T cells **(C)** from disaggregated mouse lungs 10 days after SeV challenge following pretreatment with PBS or Pam2-ODN and with or without $CD8^+$ T cells depleted on day 8 of SeV challenge. **(D)** Lung histology 10 days after SeV challenged with or without Pam2-ODN treatment and/or $CD8^+$ T cells. Data are representative of two independent experiments. Scale bar = 100 μm. n=16 mice/group for survival in experiment A and n=4 mice/group in experiment B. ****p<0.0001 compared to PBS in (c), ***p<0.0005 compared to PBS in (B) and (C), †p<0.05 compared to PBS, *p<0.05 compared to PBS.

Figure 5. Pam2-ODN inhibits SeV without altering attachment. **(A)** Flow cytometry to measure virus attachment to epithelial cells 4 h after SeV challenge. **(B)** Percentage of SeV positive epithelial cells from **(A)**. **(C)** Representative examples of immunofluorescence for virus attachment. **(D)** Mean fluorescence intensity of SeV-exposed epithelial cells 4 h after SeV challenge. **(E)** Experimental outline showing viral attachment and prevention of virus internalization by epithelial cells. **(F)** SeV M gene expression in untreated MLE-15 cells (left) or primary tracheal epithelial cells (right) challenged with liberated virus (uninternalized virus particles) from cultures that had been pretreated with PBS or Pam2-ODN prior to SeV infection 24 h after transfer of liberated virus to new cells. Data are representative of five independent experiments. *p<0.05

Figure 6. **Pam2-ODN induced reactive oxygen species protects against acute SeV virus infections and immunopathology**. SeV burden in MLE-15 cells with or without treatment with Pam2-ODN and/or NADPH inhibitors **(A)** or mitoROS inhibitors **(B)**. **(C)** SeV M gene expression in untreated MLE-15 cells challenged with liberated virus from cells that had been pretreated with PBS or Pam2-ODN with or without mitoROS inhibition. **(D)** Experimental outline. **(E)** Survival of SeV challenge in mice treated with PBS or Pam2-ODN and/or mtROS inhibitors. **(F)** Lung SeV burden measured on day 5 and **(G)** lung $CD8^+$ T cells assessed on day 10. Data are representative of three independent experiments. n=13 mice/group in experiment **D** and **E**. ***p<0.0001, **p<0.005, **p<0.01 compared to PBS, †p<0.05 compared to Pam2-ODN-treated mice without ROS inhibition, *p<0.05.

Wali, Figure 1

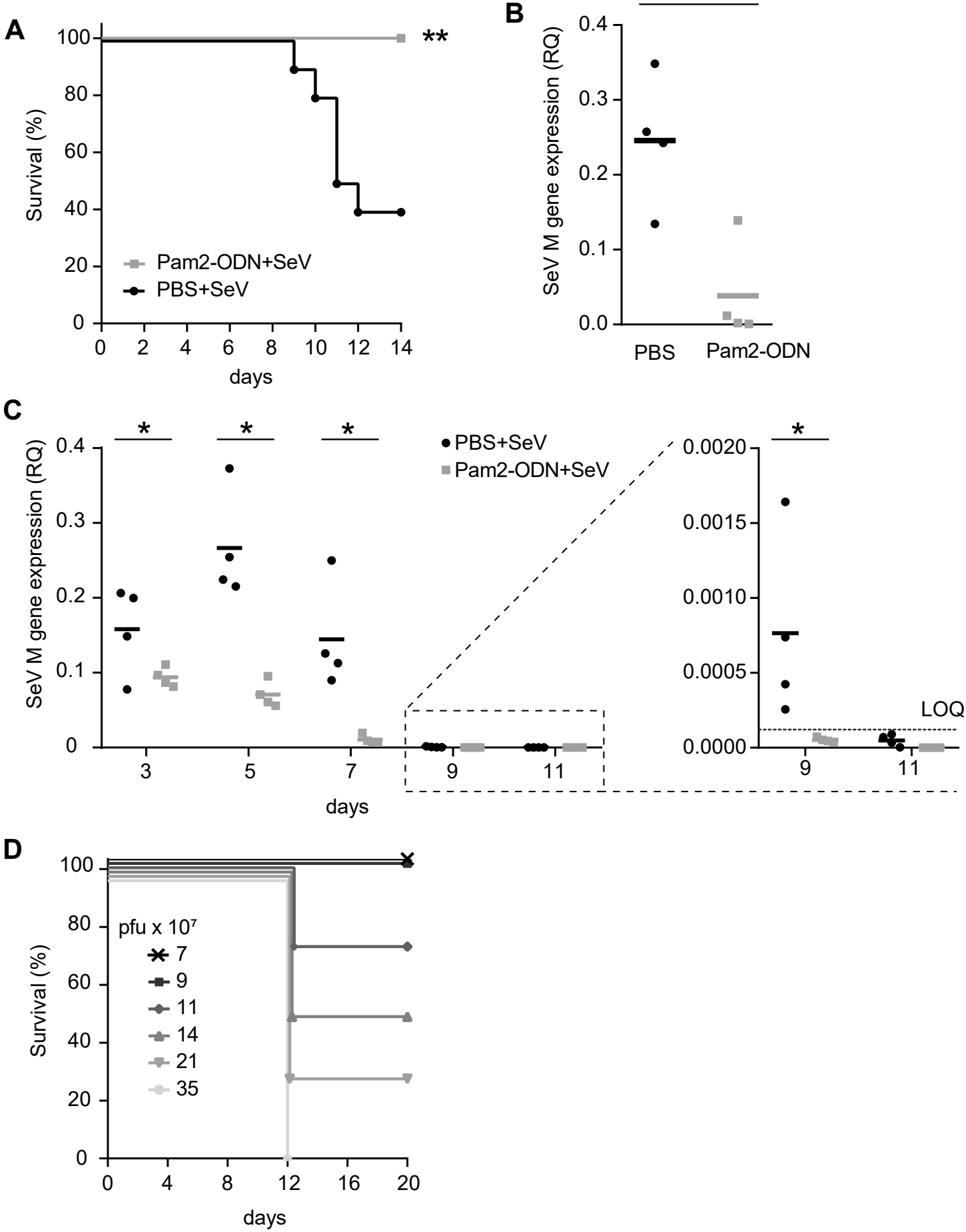

Wali, Figure 2

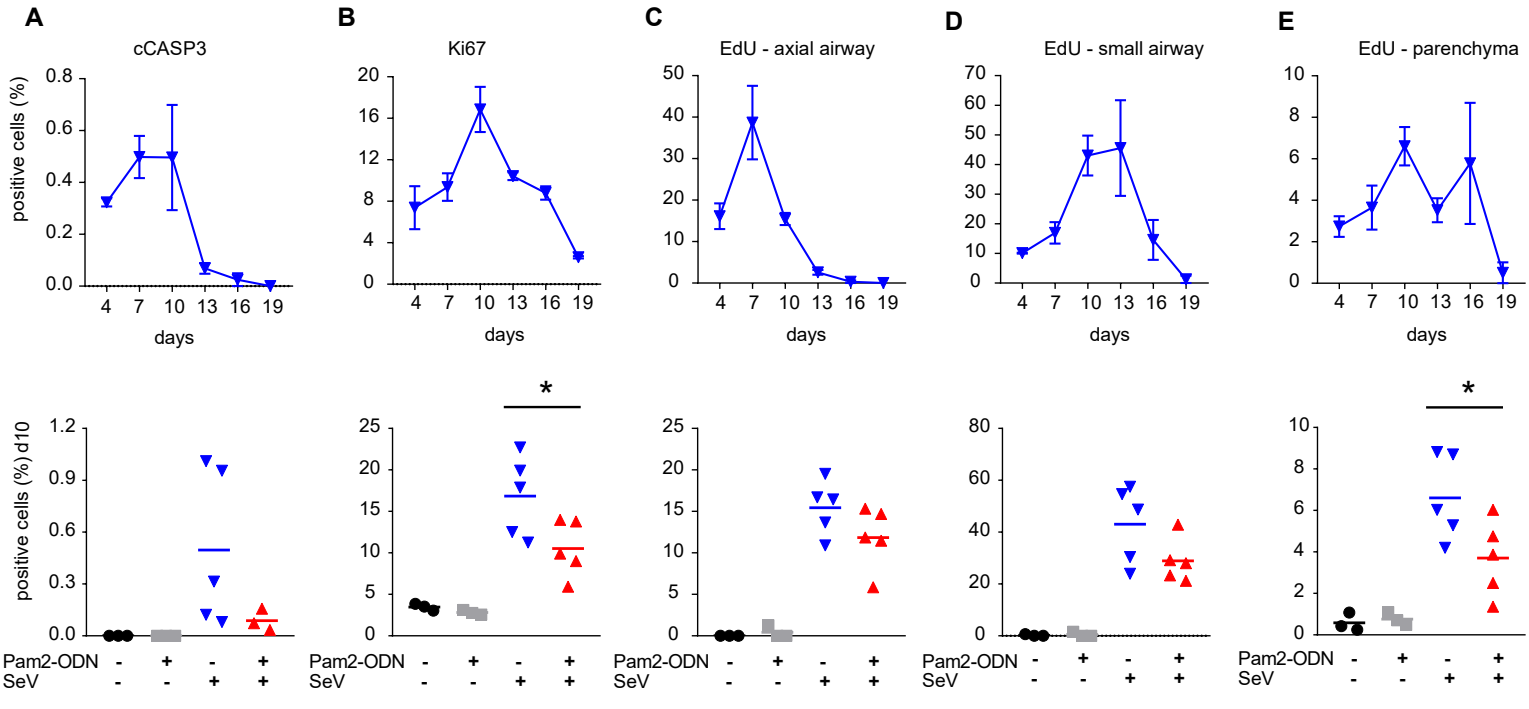

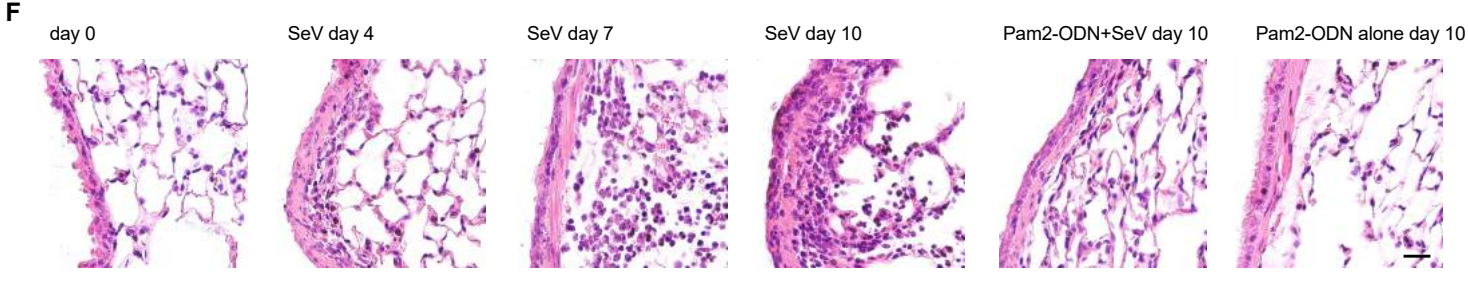

Wali, Figure 3

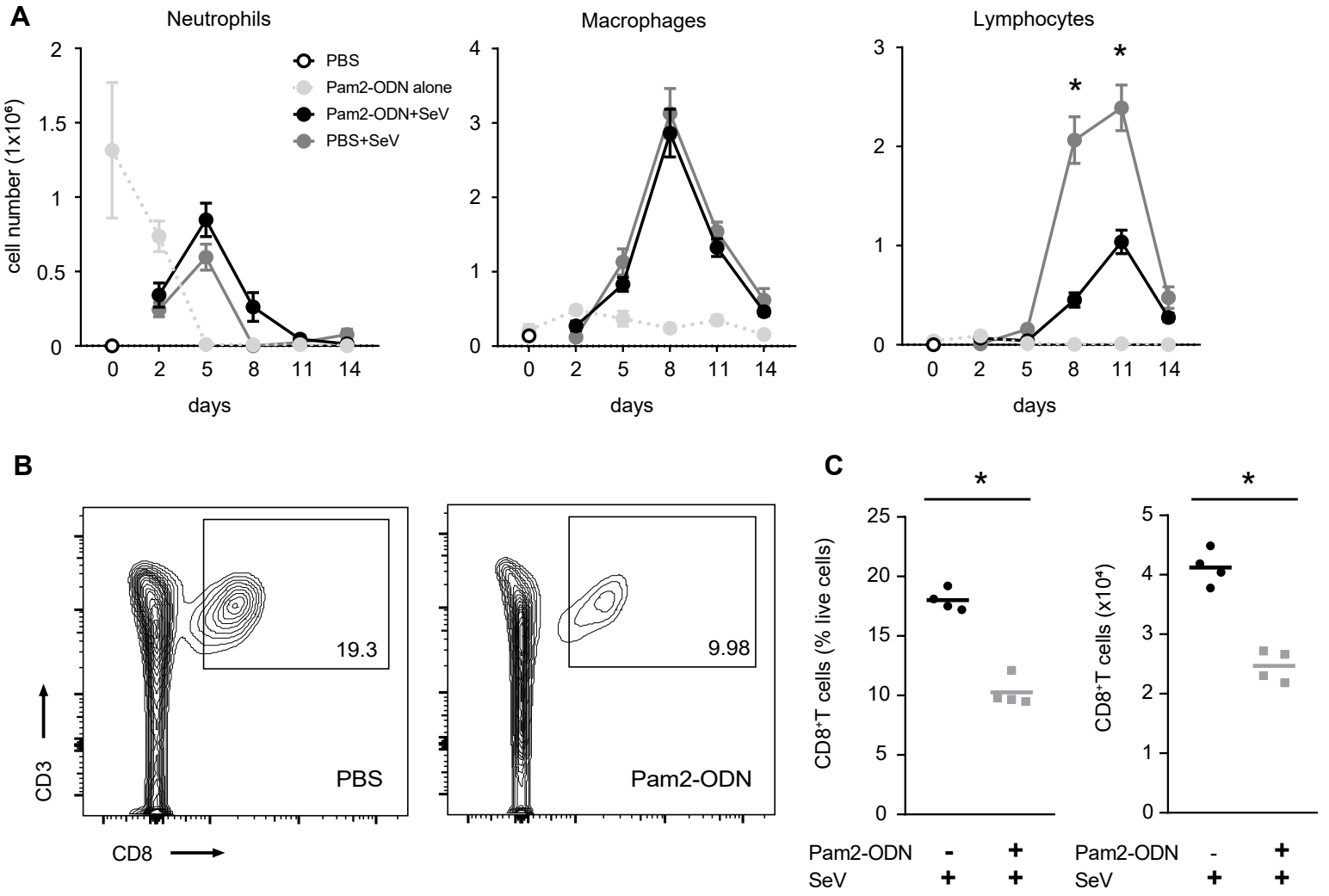

Wali, Figure 4

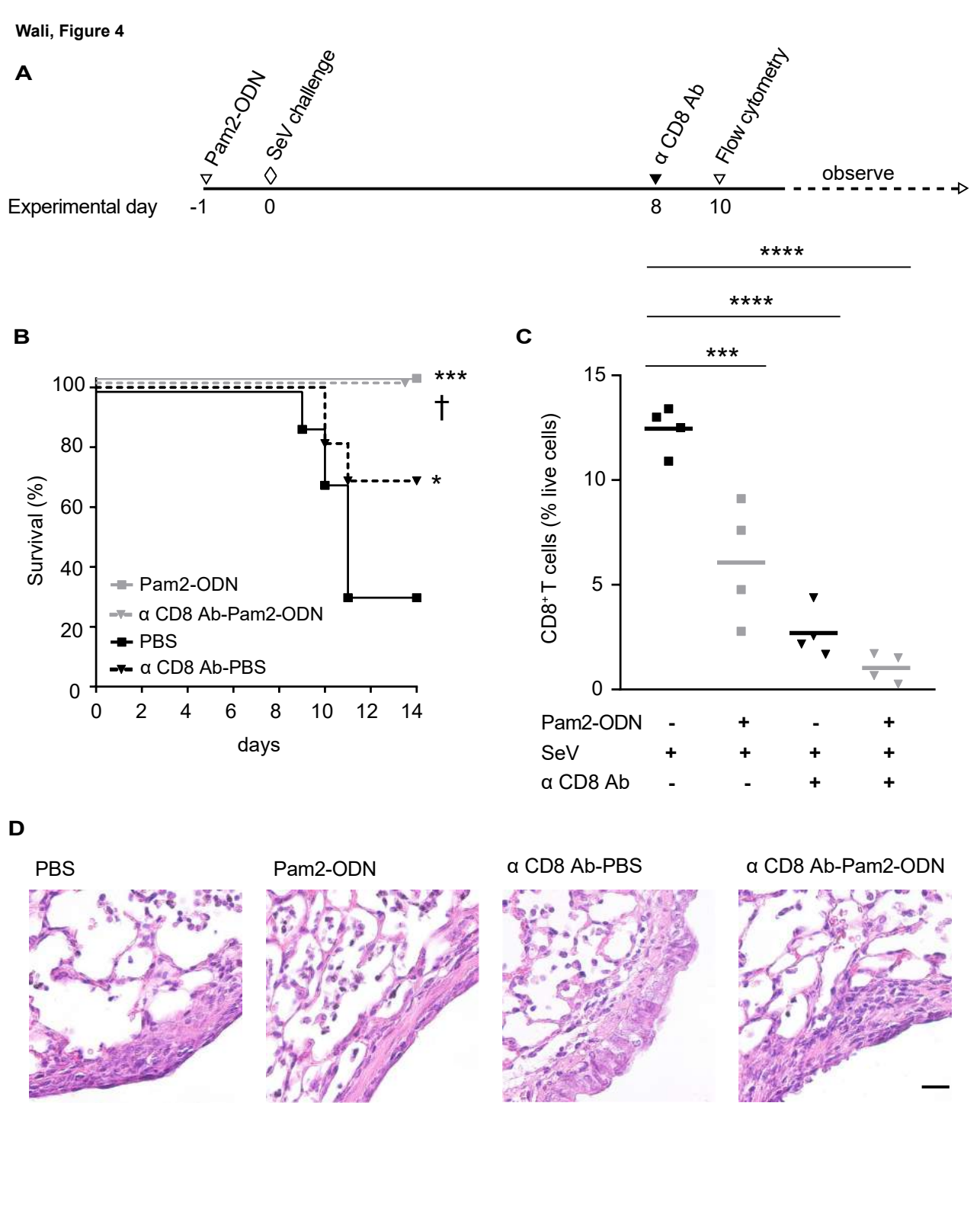

Wali, Figure 5

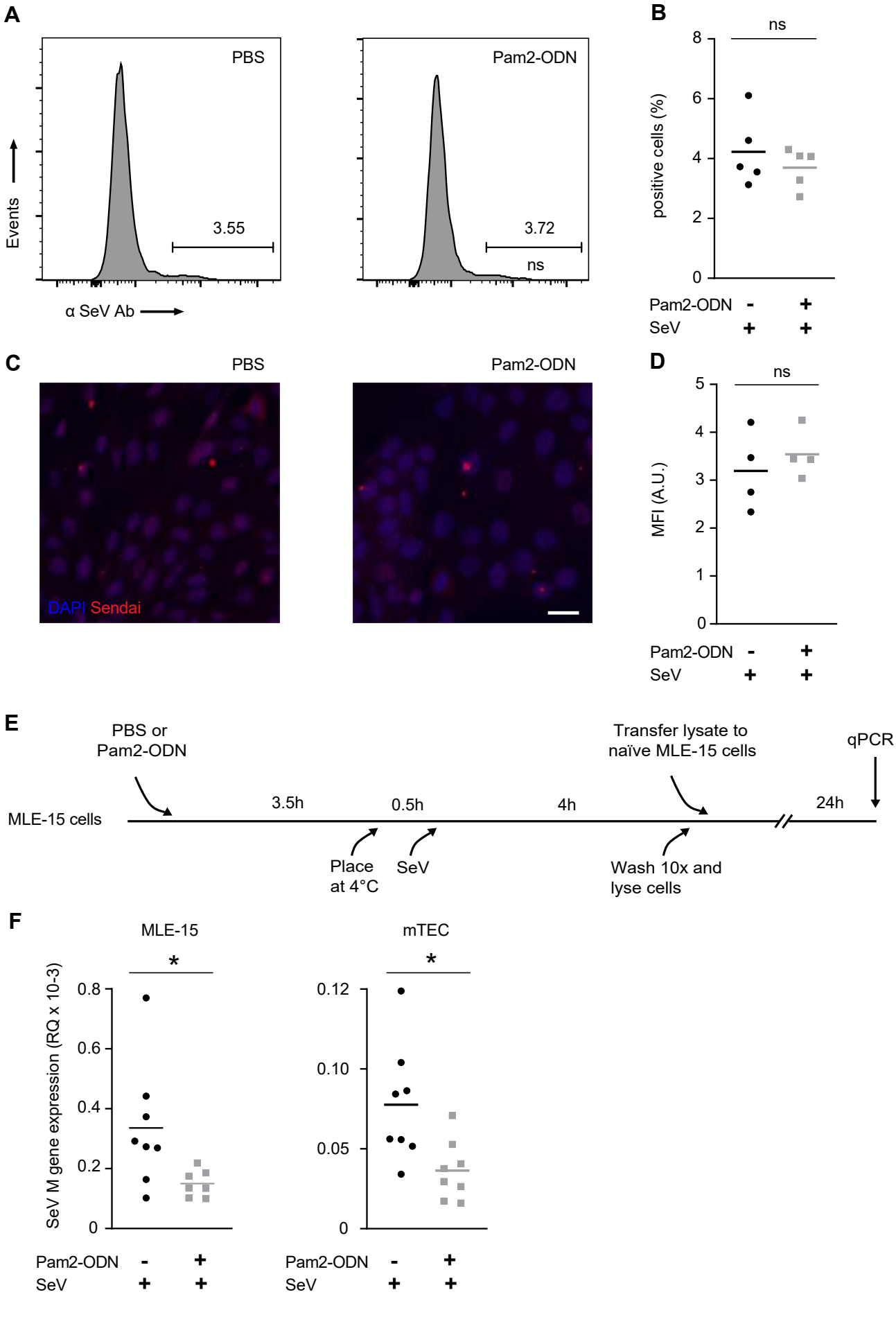

Wali, Figure 6

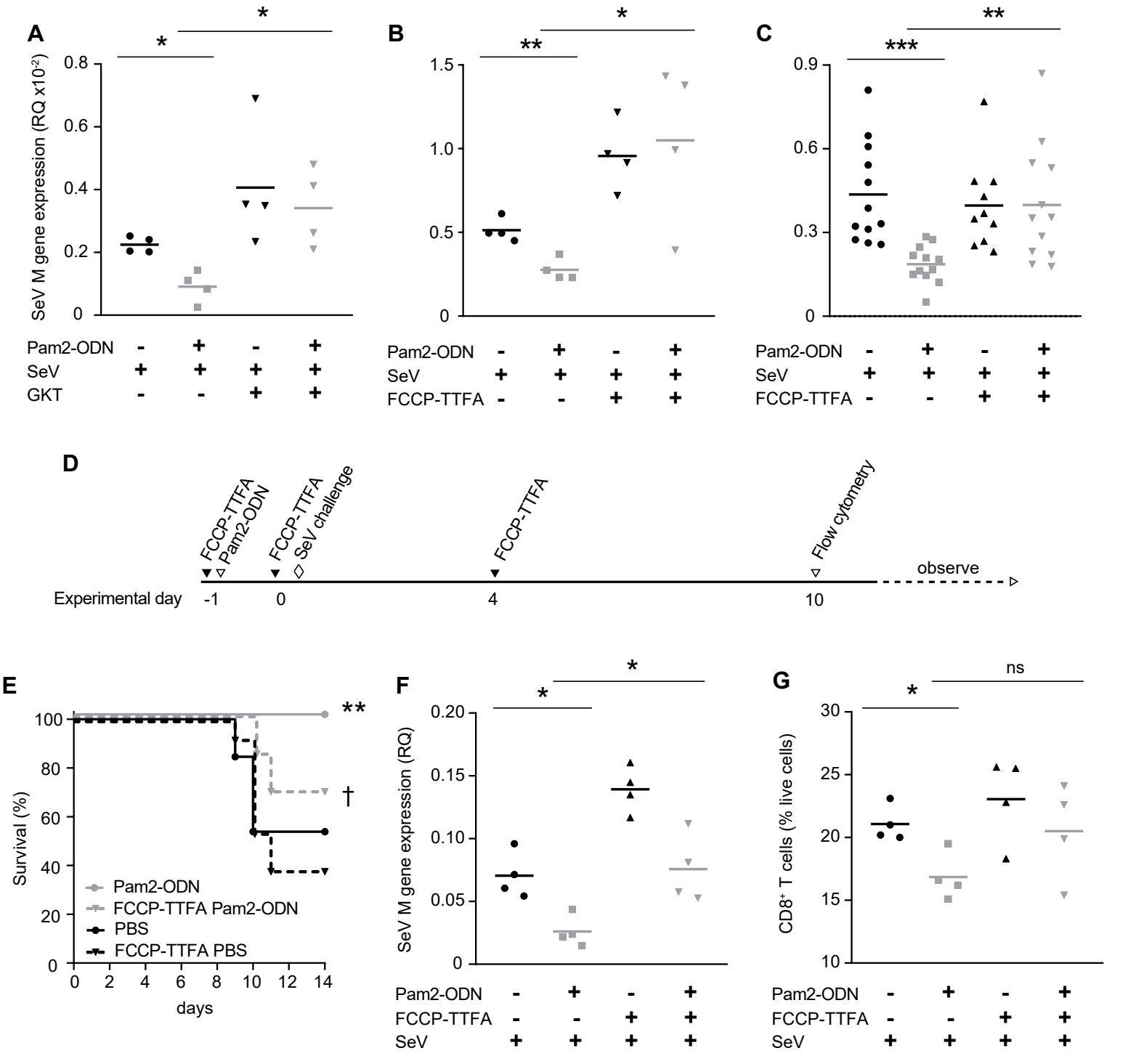

Wali, Supplemental Information

Methods

Cells: Mouse lung epithelial (MLE-15) cells were kindly provided by Jeffrey Whitsett, Cincinnati Children's Hospital Medical Center, and cultured in DMEM with 2% Fetal Bovine Serum (FBS), 1% insulin and transferrin. MLE-15 cells were authenticated by the MD Anderson Characterized Cell Line Core Facility. To harvest tracheal epithelial cells, mice were anesthetized to expose and excise tracheas. These tracheas were then digested in pronase (1.5 mg/ml, Sigma Aldrich) overnight at 4º C. Tracheal epithelial cells were then isolated and cultured on collagen coated transwells in Ham's F12 media supplemented with differentiation growth factors and hormones as previously described (1, 2).

TLR treatments and viral challenge: For *in vitro* treatments, cells were treated with $Pam2CSK_4$ (2.2 µM) and ODN M362 (0.55 µM), 4 h before SeV inoculation as previously described (2, 3). For *in vivo* treatments, 10 ml solution of $Pam2CSK_4$ (4 µM) and ODN M362 (1 µM) in endotoxin free water was delivered by Aerotech II nebulizer (Biodex Medical Systems) driven by 10 l/min along CO2 (5%) in air for 30 minutes as previously described (2, 3). SeV was purchased from ATCC (Manassas, VA) and grown in Rhesus monkey cells obtained from Cell Pro labs (Golden Valley, MN). For *in vitro* challenges, multiplicity of infection (MOI) = 1 was used. Unless otherwise stated, mice were challenged with 1×10^8 plaque forming units (pfu) in PBS inserted into the

oropharynx under isoflurane anesthesia as described (4). Mice were weighed before and daily after challenge as a measure of morbidity and criteria for euthanasia.

Viral burden quantification: Viral burden was determined by reverse transcription quantitative PCR (RT-qPCR) of the Sendai Matrix (M) protein normalized to house-keeping gene 18SRNA. For *in vivo* experiments, mouse lungs were collected 5 days after SeV challenge. RNA from mouse lungs was extracted using the Qiagen RNeasy kit. 500 ng of total RNA was converted to cDNA using Biorad iScript cDNA conversion kit. Viral burden was determined by reverse transcription quantitative PCR (RT-qPCR) of the Sendai Matrix (M) protein normalized to house-keeping gene 18SRNA. 18S forward primer – GTAACCCGTTGAACCCCATT; reverse primer – CCATCCAATCGGTAGTAGCG. SeV M gene forward primer – ACTGGGACCCTATCTAAGACAT; reverse primer – TAGTAGCGGAAATCACGAGG. The Limit of quantification (LOQ) was established for the SeV qPCR assay as the highest dilution of the template still maintaining the linearity of the assay. The threshold cycle (C_T) value of the LOQ was set as the lower limit for the assay.

Flow cytometry: For *in vivo* experiments, mouse lungs were perfused with 5 to 10 ml PBS, dissected, cut into 1 mm^3 pieces, and digested with collagenase/DNAse I (5 mg/ml, Worthington biochemical) for 30 min at 37° C. After digestion, single cells were collected by passing through a 70 µm filter. These single cells were washed with FACS staining buffer (PBS supplemented with 1% FBS) and stained for specific cell types, as indicated in the antibody table (Table 1). For *in vitro* experiments, MLE-15 cells were seeded on 24 well plates for treatment with Pam2-ODN and SeV inoculation. Cells were

trypsinized and washed with FACS staining buffer 2X. Cells were blocked in 5% donkey serum for 30 min before proceeding to staining with Rabbit SeV antibody (MBL International) overnight at 4° C, followed by staining with secondary Alexa488 anti-rabbit antibody (Jackson Immunologicals) for 1 h. Cells were fixed and acquired on a BD LSRII (BD Biosciences) for Alexa488 positive cells.

Epithelial proliferation assays: Mice were injected intraperitoneally with 0.1 ml EdU (1 mg/mouse). After 24 h, lungs were inflated and fixed with 10% formalin for 24 h at 4° C and then lungs were embedded in paraffin. Paraffin sections were cut into 5 µm transverse sections of the axial airway, between lateral branches 1 and 2. Lung sections were then stained following the Click-iT EdU Imaging Kit protocol for EdU (Abcam) followed by staining with DAPI for 30 min at room temperature. Images were collected using Olympus BX60 microscope using identical parameters for all conditions. Some lung sections were subjected to antigen retrieval and then stained for Ki67 (1:1000; Invitrogen) or cCasp3 (1:500; Cell Signaling). EdU, Ki67 or cCasp3 positive cells were quantified using a cell counter plugin in ImageJ and normalized to DAPI positive cells in every field of view (number of fields surveyed per mouse sample = 3).

Bronchoalveolar lavage and differential Giemsa staining: After deep anesthesia, mouse tracheas were exposed, cannulated with a 20-gauge syringe, and instilled with 1.5 ml of PBS. Approximately 1 ml of BAL fluid was collected per sample. The BAL fluid was then spun down at 4º C at 300 *g* to collect the cells in the pellet. The cell pellet was resuspended in 1 ml of ice-cold PBS and 200 µl of this cell suspension was then

subjected to cytocentrifugation at 300 *g* for 5 min. Cells were stained with Giemsa stain for differential count determination and total cells were counted by hemocytometer.

Immunofluorescence microscopy for SeV: MLE-15 cells were grown on chamber slides (Labtek), treated with Pam2-ODN for 4 h before inoculation with SeV (MOI 1). Cells were then fixed with 2% paraformaldehyde before staining with rabbit anti-SeV antibody (MBL International) and detected using a secondary anti-rabbit antibody. For each experimental condition, specimens were imaged using Olympus BX60 microscope using identical parameters for time of exposure, color intensity, contrast and magnification. Images were then loaded on ImageJ software to calculate mean fluorescence intensity for each group.

Hematoxylin and eosin staining: Mouse lungs were fixed by intratracheal inflation with 10% formalin for 24 h, and then transferred to 70% ethanol embedded in paraffin. Tissue blocks were then cut into 5 µm sections, mounted onto frosted glass slides, deparaffinized with xylene, washed with ethanol, then rehydrated and stained with hematoxylin and eosin for morphological changes.

Viral attachment assays: MLE-15 cells were cultured in 24 well plates or chamber slides for treatment with Pam2-ODN and SeV inoculations. The cells were infected with SeV at 4º C for 4 hours. Thereafter, the cells were vigorously washed 5X with media to remove unattached virus, then harvested to measure uninternalized SeV burden using immunofluorescence or flow cytometry. For RT-qPCR assays, epithelial cells were

treated with Pam2-ODN or PBS, followed by SeV infection at 4º C to prevent virus internalization. Virus particles were allowed to attach to the epithelial targets for 4 h at 4º C. These cells were then extensively washed to remove unattached virus particles, and then the cells were lysed by passing through a syringe 10X to liberate the attached uninternalized virus particles. The liberated virus particles were then transferred to naïve epithelial cells that had no prior exposure to Pam2-ODN. SeV M gene expression was assessed by qPCR after 24 h of SeV replication in the new cells. In some experiments, mitoROS inhibitors (FFCP-TTFA) were used before Pam2-ODN treatment to determine the role of Pam2-ODN induced ROS in SeV inactivation prior to epithelial internalization.

ROS inhibition *in vitro* and *in vivo*: NADPH oxidase activity was inhibited by exposing the cells to GKT137831 (10 µM; Selleckchem) 12 h prior to treatment with Pam2-ODN or PBS. Mitochondrial ROS production was inhibited using the combination of FCCP (400 nM, Cayman Chemicals) and TTFA (200 µM, Cayman Chemicals) for 1 h before Pam2-ODN or PBS treatment. For *in vivo* experiments, mice were aerosolized with 10 ml TTFA (200 mM) and FCCP (800 µM) 2 h before Pam2-ODN aerosolization and 2 h before SeV challenge and then again 4 days after SeV challenge.

Statistics: All statistical analysis was performed using GraphPad Prism software (Version 8 for Windows, GraphPad Software, La Jolla, CA). Data from one representative experiment of at least three independent experiments are presented as mean +/- standard error of biological replicates. To determine pairwise differences in

viral burden or cell numbers, Student's *t* test was used. Mouse survival analysis of viral challenges were analyzed using Mantel-Cox test. One-way analysis of variance (ANOVA) with multiple comparisons was used to determined differences between multiple experimental conditions.

References:

1. Leiva-Juarez MM, Ware HH, Kulkarni VV, Zweidler-McKay PA, Tuvim MJ, Evans SE. Inducible epithelial resistance protects mice against leukemia-associated pneumonia. *Blood* 2016;128(7):982-992.

2. Kirkpatrick CT, Wang Y, Leiva Juarez MM, Shivshankar P, Pantaleon Garcia J, Plumer AK, Kulkarni VV, Ware HH, Gulraiz F, Chavez Cavasos MA, et al. Inducible lung epithelial resistance requires multisource reactive oxygen species generation to protect against viral infections. *mBio* 2018;9(3).

3. Ware HH, Kulkarni VV, Wang Y, Pantaleon Garcia J, Leiva Juarez M, Kirkpatrick CT, Wali S, Syed S, Kontoyiannis AD, Sikkema WKA, et al. Inducible lung epithelial resistance requires multisource reactive oxygen species generation to protect against bacterial infections. *PLoS One* 2019;14(2):e0208216.

4. Goldblatt DL, Flores JR, Valverde Ha G, Jaramillo AM, Tkachman S, Kirkpatrick CT, Wali S, Hernandez B, Ost DE, Scott BL, et al. Inducible epithelial resistance against acute sendai virus infection prevents chronic asthma-like lung disease in mice. *British journal of pharmacology* 2020.

Supplementary figures:

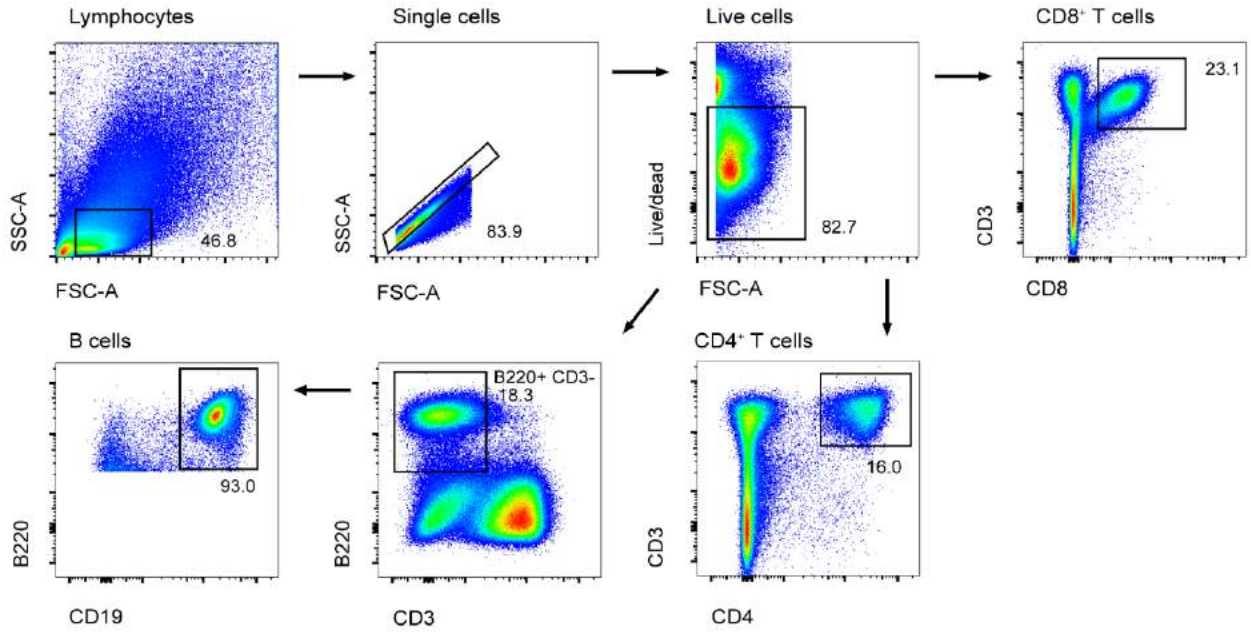

Supplementary Figure 1. Gating strategy for flow cytometry of lung T and B cells.

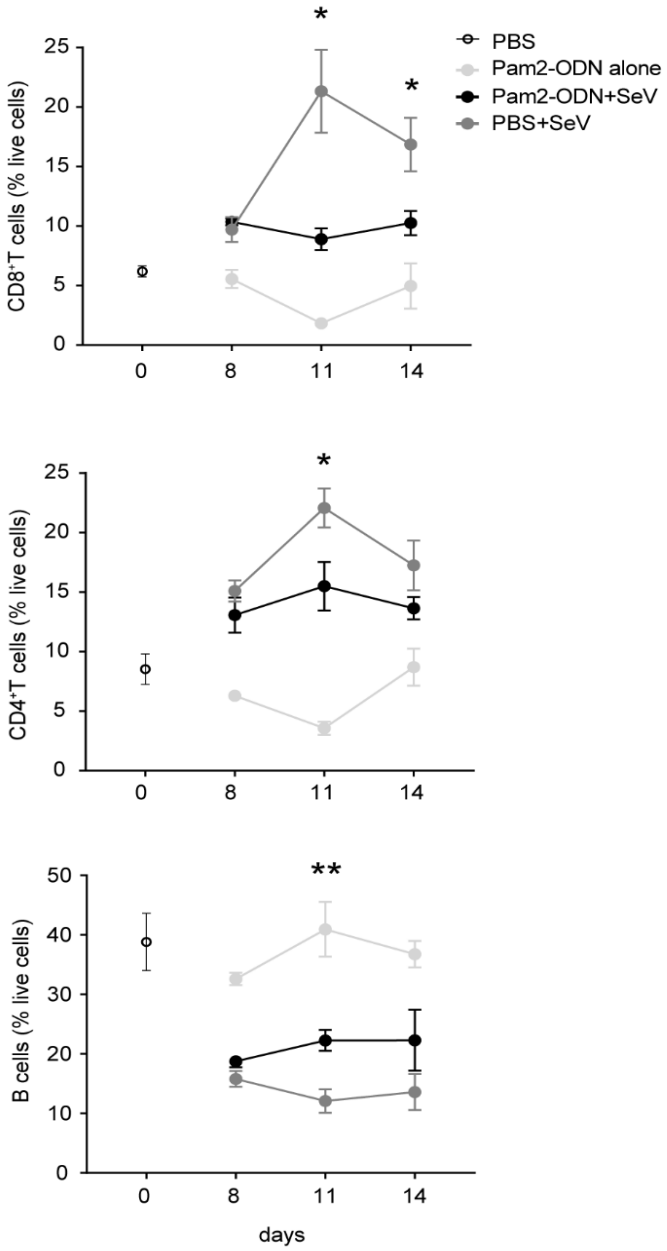

Supplementary Figure 2. Pam2-ODN pretreatment reduced SeV induced lymphocytes. Disaggregated mouse lung cells positive for $CD8^+$ T cells, $CD4^+$ T cells, $CD19^+$ $B220^+$ B cells assessed by flow cytometry in perfused lungs from mice treated with PBS or Pam2-ODN on various days of SeV challenge. Data are representative of three independent experiments. *p<0.05 compared to PBS+SeV, **p<0.01 compared to PBS+SeV.

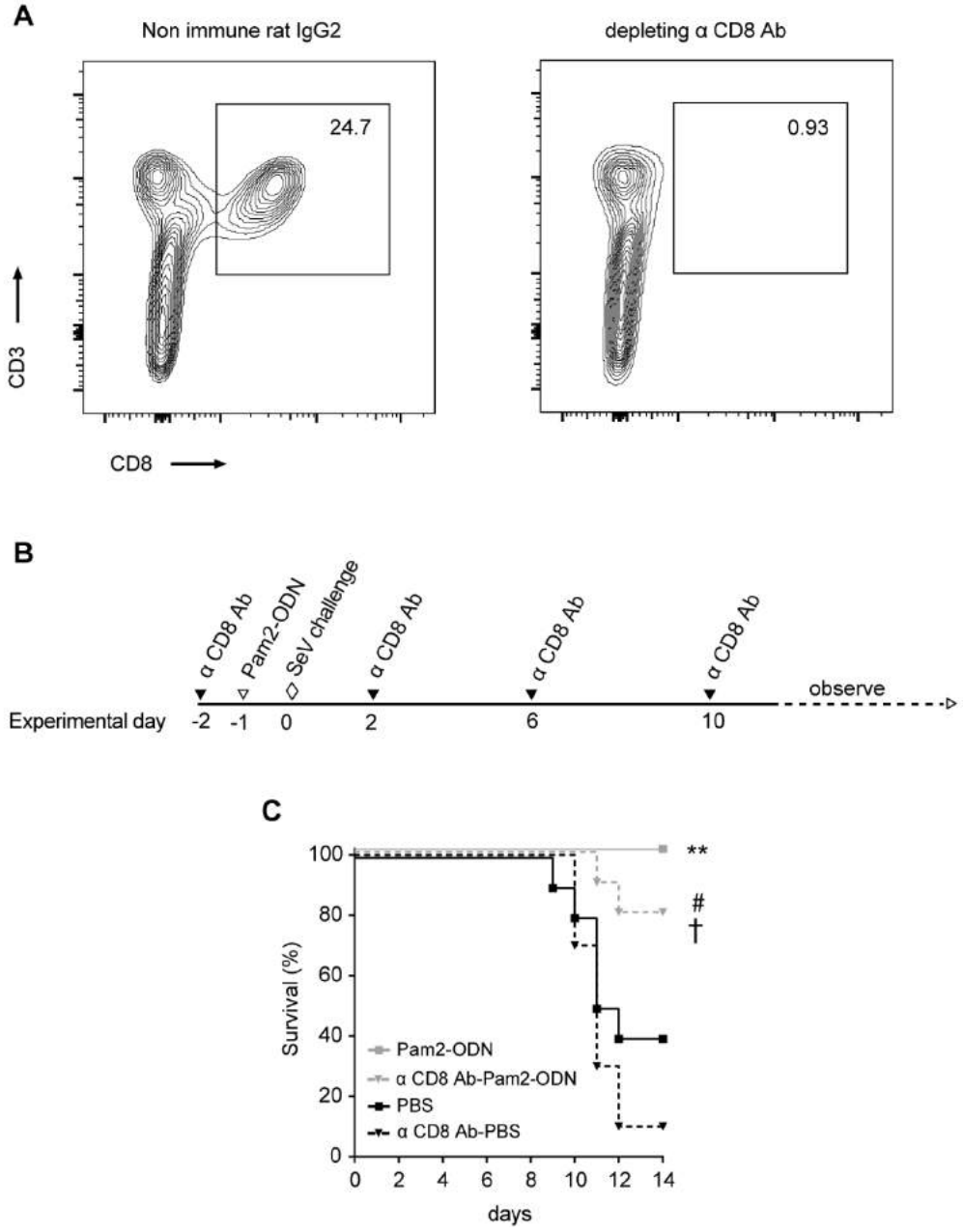

Supplementary Figure 3. CD8⁺T cell depletion in mice. (A) Flow cytometry of CD8⁺T cells to confirm depletion of CD8+T cells by depleting antibody. Experimental outline **(B)**, survival **(C)** of mice SeV challenge following PBS or Pam2-ODN treatment and with or without preinfection CD8⁺ T cell depletion. ***p*<0.005 compared to PBS, #*p*<0.005 compared to α CD8 Ab-PBS, †*p*<0.05 compared to PBS.

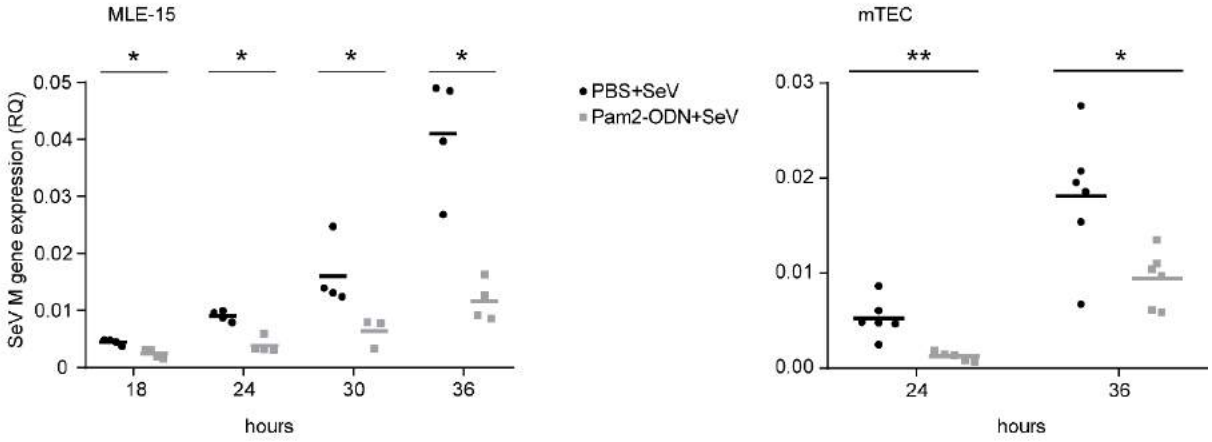

Supplementary Figure 4. Pam2-ODN pretreatment reduced SeV burden in isolated lung epithelial cells. SeV burden assessed by qPCR in MLE-15 cells and primary mouse tracheal epithelial cells (mTEC) treated with PBS or Pam2-ODN 4h prior to SeV challenge. Data are representative of four independent experiments. *p<0.05, **p<0.005 compared to PBS treated group.